Rhenium(I) tricarbonyl complexes with bispyridine ligands attached to sulfur-rich core: Syntheses, structures and properties

Ya Chen [a], Wei Liu [a], Jian-Shi Jin [a], Bin Liu [b], Zhi-Gang Zou [b], Jing-Lin Zuo [a,*], Xiao-Zeng You [a]

[a] Coordination Chemistry Institute and The State Key Laboratory of Coordination Chemistry, School of Chemistry and Chemical Engineering, Nanjing University, Han Kou Road, Nanjing 210093, PR China
[b] National Laboratory of Solid State Microstructure, Nanjing University, Nanjing 210093, PR China

ABSTRACT

Rhenium(I) tricarbonyl complexes with bispyridine ligands bearing sulfur-rich pendant, $Re(CO)_3(Medpydt)X$ (Medpydt = dimethyl 2-(di(2-pyridyl)methylene)-1,3-dithiole-4,5-dicarboxylate; X = Cl, **1**; X = Br, **2**) and $Re(CO)_3(MebpyTTF)X$ (MebpyTTF = 4,5-bis(methyloxycabonyl)-4′,5′-(4′-methyl-2,2′-dipyrid-4-ylethylenedithio)-tetrathiafulvalene; X = Cl, **5**; X = Br, **6**), were prepared from the reactions between $Re(CO)_5X$ (X = Cl, Br) and Medpydt or MebpyTTF, respectively. Hydrolysis of the above complexes afforded the analogues with carboxylate derivatives, $Re(CO)_3(H_2dpydt)X$ (X = Cl, **3**; X = Br, **4**) and $Re(CO)_3(H_2bpyTTF)X$ (X = Cl, **7**; X = Br, **8**). The crystal structures for complexes **1** · 2H_2O, **5** and **6** were determined using X-ray single crystal diffraction. UV–Vis absorption spectra of the rhenium complexes show the intraligand and MLCT transitions. Electrochemical behaviors of all new compounds were studied with cyclic voltammetry. Upon irradiation, complexes **3–6** exhibit blue to red emissions in fluid solutions at the room temperature. The performance of complexes **3**, **4**, **7** and **8** as photosensitizers for anatase TiO_2 solar cells was preliminarily investigated as well.

1. Introduction

Considerable efforts have been devoted to the design and synthesis of transition-metal polypyridine complexes, largely due to their potential applications such as efficient photocatalysts for CO_2 reduction [1–6], materials for molecular electronics and photonics [7–18], and sensitizers for solar energy conversion [19–28]. In the dye-sensitized solar cells (DSSCs) based on Ru[II] polypyridyl dyes, carboxylic acid pendants are key to the attachment of dyes to the semiconductor surface [29]. Significant progress has been made in the research of Ru[II] polypyridyl sensitizers with carboxylate in DSSCs [24–32]. Similar to ruthenium compounds, rhenium polypyridine complexes containing a *fac*-{Re(CO)_3}⁺ core are attractive research targets owing to their intriguing photophysical, photochemical, excited-state redox properties, and potential role as a dye for DSSC application [33–41]. However, there are only limited studies exploring the photovoltaic performance of tricarbonyl rhenium(I) complexes with carboxylic pendants in DSSCs [42].

The 1,3-dithiole ligands incorporating bispyridine are promising candidates for constructing novel molecular structures with attractive properties and potential applications [43–47]. In our group, a continuous research effort has been mainly focused on rhenium(I) complexes with ligands containing di(2-pyridyl) and

1,3-dithiole moieties [48–49]. Tetrathiafulvalene (TTF) and its derivatives derived from 1,3-dithiole have received much attention for decades, on account of their highly desirable properties and growing utility as versatile building blocks in molecular, supramolecular and materials chemistry [50–56]. To the best of our knowledge, there is no literature precedent of tricarbonyl rhenium(I) complex containing TTF unit.

In this paper, we successfully prepared a series of rhenium(I) tricarbonyl complexes with bispyridine ligands incorporating with 1,3-dithiole units, namely $Re(CO)_3(Medpydt)X$ and $Re(CO)_3(H_2dpydt)X$ (X = Cl and Br) (Chart 1). As a comparison, we also synthesized rhenium(I) tricarbonyl complexes containing TTF derivatives, $Re(CO)_3(MebpyTTF)X$ and $Re(CO)_3(H_2bpyTTF)X$ (X = Cl and Br) (Chart 1). The structures, photochemical and electrochemical behaviors have been discussed. Furthermore, the photovoltaic performance of $Re(CO)_3(H_2dpydt)X$ and $Re(CO)_3(H_2bpyTTF)X$ (X = Cl and Br) containing carboxylic groups as photosensitizers in the nanocrystalline TiO_2-based solar cells are studied.

2. Results and discussion

2.1. Syntheses and characterizations

Both dimethyl 2-(di(2-pyridyl)methylene)-1,3-dithiole-4,5-dicarboxylate (**L¹**) and 4,5-bis(methyloxycabonyl)-4′,5′-(4′-methyl-2,2′-dipyrid-4-ylethylenedithio)-tetrathiafulvalene (**L²**) were

* Corresponding author. Tel.: +86 25 83593893; fax: +86 25 83314502.
E-mail address: zuojl@nju.edu.cn (J.-L. Zuo).

X = Cl, R = Me, **1**; X = Cl, R = H, **3**
X = Br, R = Me, **2**; X = Br, R = H, **4**

X = Cl, R = Me, **5**; X = Cl, R = H, **7**
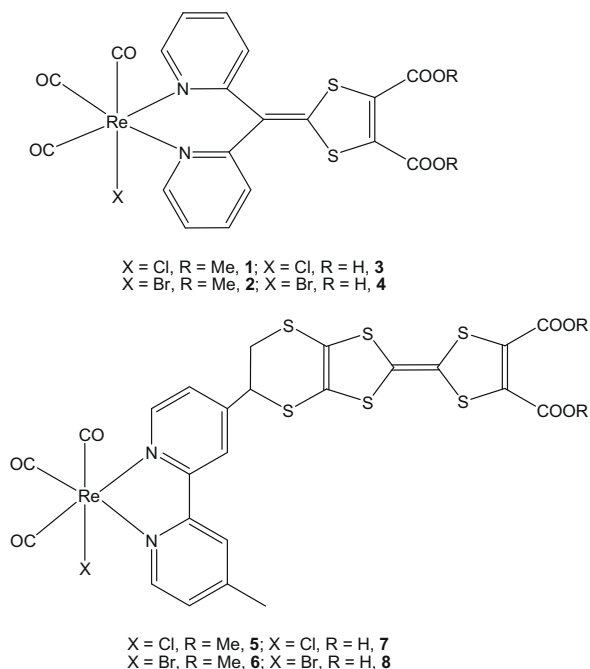X = Br, R = Me, **6**; X = Br, R = H, **8**

Chart 1.

synthesized by the standard triethyl phosphite-mediated cross-coupling reaction. All rhenium(I) complexes containing ester groups were prepared in good yields by refluxing equivalent amounts of the ligand and Re(CO)$_5$X (X = Cl, Br) in toluene for a few hours. Finally, hydrolysis of the compounds containing ester group afforded the corresponding complexes with carboxylic acid (Schemes 1 and 2).

The IR spectra of these Re^I complexes show three strong bands in the absorption region of 1875–2020 cm^{-1}, which are related to a *facial* arrangement of the three carbonyl groups in the coordination sphere [57–59].

The results from mass spectra for all complexes are consistent with the formulations from elemental analysis and the spectroscopy. For instance, in the MALDI-TOF mass spectrum of Re(CO)$_3$(Medpydt)Cl (**1**), the most prominent m/z peak occurs at 657.1, which corresponds to [Re(CO)$_3$(Medpydt)]$^+$.
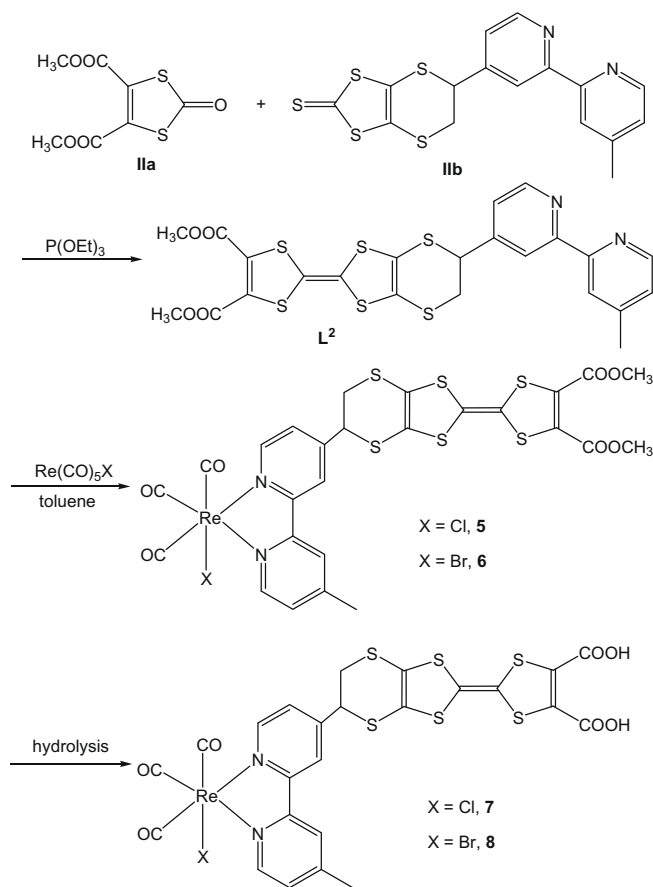
Scheme 2. Synthetic routes of compounds **L^2** and **5–8**.

2.2. Structural description

The crystallographic data for the rhenium complexes **1** · 2H$_2$O, **5** and **6** are listed in Table 1. Selected bond lengths and angles are given in Table 2. Figs. 1 and 2 and Fig. S1 depict the perspective drawings of **1** · 2H$_2$O, **5** and **6** with atomic numbering, respectively. All the structures show the chemically robust *fac*-{Re(CO)$_3$}$^+$ core and distorted octahedral geometries.

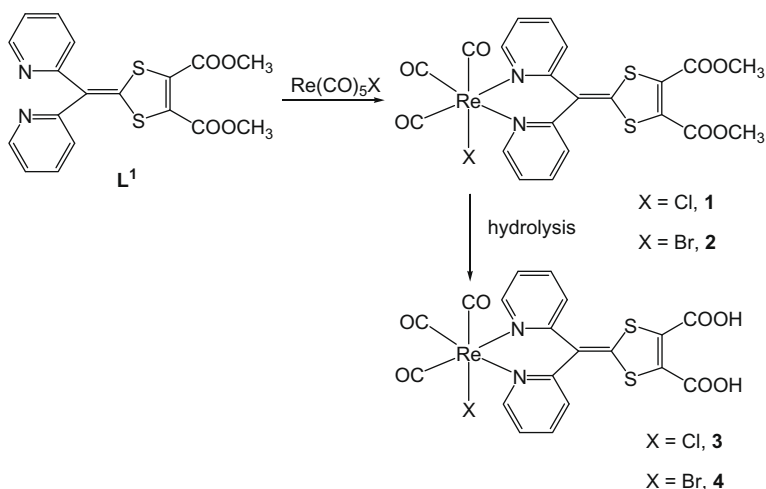**Scheme 1.** Synthetic routes of compounds **1–4**.

Table 1
Crystal data and structure refinement for complexes $1 \cdot 2H_2O$, **5** and **6**.

	$1 \cdot 2H_2O$	**5**	**6**
Empirical formula	$ReC_{21}H_{18}ClN_2O_9S_2$	$ReC_{26}H_{18}ClN_2O_7S_6$	$ReC_{26}H_{18}BrN_2O_7S_6$
M_r	728.14	884.43	928.89
Temperature (K)	293(2)	293(2)	293(2)
Crystal system	Triclinic	Monoclinic	Monoclinic
Space group	$P\bar{1}$	$P2_1/c$	$P2_1/c$
a (Å)	9.045(2)	14.0990(15)	14.0768(19)
b (Å)	12.519(3)	15.7280(18)	15.843(2)
c (Å)	13.074(3)	14.3195(16)	14.528(2)
α (°)	100.063(4)	90	90
β (°)	107.520(4)	101.376(2)	101.787(3)
γ (°)	95.710(5)	90	90
V (Å^3)	1371.7(5)	3113.0(6)	3171.5(8)
Z	2	4	4
D (g/cm^3)	1.763	1.887	1.945
μ (Mo Kα) (mm^{-1})	4.728	4.439	5.533
$F(000)$	708	1728	1800
θ range (°)	1.67–26.00	1.94–28.32	1.92–25.00
Reflections collected	7422	18361	15513
Independent reflections [$R_{(int)}$]	5258 [0.1221]	7299 [0.1192]	5589 [0.0990]
Data/restraints/ parameters	5258/0/326	7299/14/391	5589/35/388
GOF on F^2	0.959	1.244	0.861
R_1[a], wR_2[b] [$I > 2\sigma(I)$]	0.0680, 0.1700	0.1095, 0.2418	0.0624, 0.1239
R_1[a], wR_2[b] (all data)	0.0875, 0.1769	0.1353, 0.2570	0.1272, 0.1423
Largest difference peak and hole (e Å^{-3})	2.518/1.930	3.601/1.270	1.921/0.755

[a] $R_1 = \Sigma||C| - |F_c||/\Sigma F_o|$.
[b] $wR_2 = [\sum w(F_o^2 - F_c^2)^2 / \sum w(F_o^2)]^{1/2}$.

Table 2
Selected bond lengths [Å] and angles [°] for complexes $1 \cdot 2H_2O$, **5** and **6**.

$1 \cdot 2H_2O$

Re(1)–C(1)	1.857(17)	N(1)–Re(1)–N(2)	83.2(3)
Re(1)–C(2)	1.879(14)	C(2)–Re(1)–N(1)	174.0(5)
Re(1)–C(3)	1.889(13)	C(3)–Re(1)–N(2)	177.9(5)
Re(1)–N(1)	2.206(9)	C(1)–Re(1)–Cl(1)	175.6(5)
Re(1)–N(2)	2.207(9)	O(1)–C(1)–Re(1)	173.8(13)
Re(1)–Cl(1)	2.473(4)	O(2)–C(2)–Re(1)	177.1(13)
C(14)–C(15)	1.313(16)	O(3)–C(3)–Re(1)	177.3(14)

5

Re(1)–C(1)	1.860(14)	N(1)–Re(1)–N(2)	75.0(4)
Re(1)–C(2)	1.897(17)	C(1)–Re(1)–N(2)	173.5(7)
Re(1)–C(3)	1.928(15)	C(3)–Re(1)–N(1)	175.1(5)
Re(1)–N(1)	2.165(11)	C(2)–Re(1)–Cl(1)	175.7(5)
Re(1)–N(2)	2.152(9)	O(1)–C(1)–Re(1)	176(2)
Re(1)–Cl(1)	2.482(5)	O(2)–C(2)–Re(1)	178.0(18)
C(19)–C(20)	1.332(17)	O(3)–C(3)–Re(1)	175.4(18)
C(15)–C(16)	1.438(10)	C(1)–Re(1)–C(2)	86.7(11)
C(17)–C(18)	1.315(19)	C(1)–Re(1)–C(3)	86.1(8)

6

Re(1)–C(1)	1.952(15)	N(1)–Re(1)–N(2)	75.5(4)
Re(1)–C(2)	1.802(13)	C(1)–Re(1)–N(1)	173.2(5)
Re(1)–C(3)	1.984(5)	C(3)–Re(1)–N(2)	171.9(5)
Re(1)–N(1)	2.116(10)	C(2)–Re(1)–Br(1)	173.4(6)
Re(1)–N(2)	2.116(10)	O(1)–C(1)–Re(1)	179.1(13)
Re(1)–Br(1)	2.6080(18)	O(2)–C(2)–Re(1)	159(2)
C(19)–C(20)	1.359(14)	O(3)–C(3)–Re(1)	177.2(16)
C(15)–C(16)	1.417(9)	C(2)–Re(1)–C(1)	91.3(6)
C(17)–C(18)	1.306(15)	C(2)–Re(1)–C(3)	84.9(7)

In complex $1 \cdot 2H_2O$, the two aromatic rings form a "butterfly-like" substructure due to the flexibility of the di(2-pyridyl) moiety. The *trans* angles (C(2)–Re(1)–N(1), C(3)–Re(1)–N(2), and C(1)–Re(1)–Cl(1)) are in the range of 174.0(5)–177.9(5)° and the angle of N1–Re–N2 is 83.2(3)°, showing only minor deviations from the idealized octahedral limit. The bond lengths of rhenium carbonyl
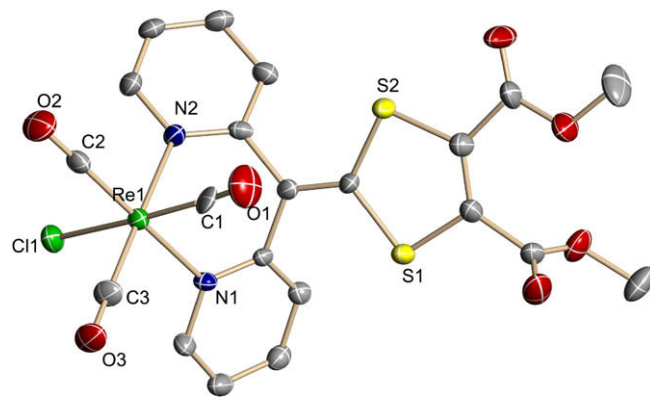
Fig. 1. ORTEP view of $1 \cdot 2H_2O$ with atom numbering scheme: hydrogen atoms and water molecules are omitted for clarity. Ellipsoids are drawn at the 30% probability level.
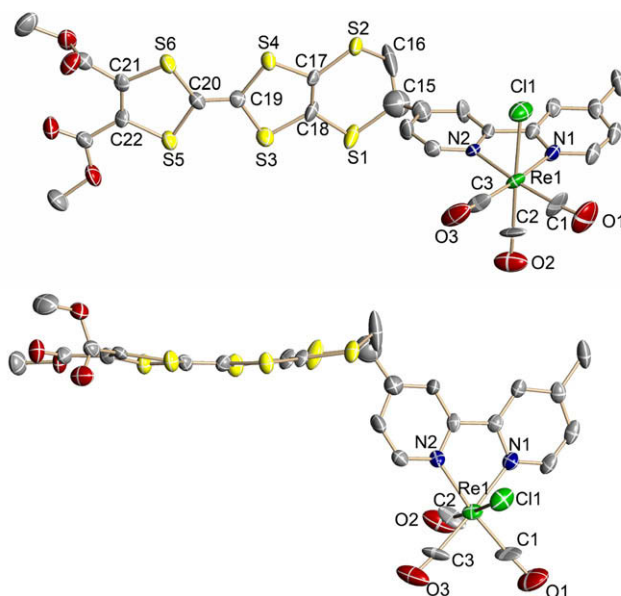
Fig. 2. ORTEP view of **5** with atom numbering scheme (including top and side views of TTF unit): hydrogen atoms are omitted for clarity. Ellipsoids are drawn at the 30% probability level.

(1.857(17) 1.889(13) Å) and Re–Cl (2.473(4) Å) are consistent with those found in similar tricarbonyl rhenium(I) complexes. The rhenium–nitrogen distances are almost identical (2.206(9) Å and 2.207(9) Å), which are in good agreement with the relatively symmetrical structure of ligand Medpydt.

Complexes **5** and **6** containing TTF unit are very similar in the structure, with the exception that the halide ligand for complex **5** is Cl while for **6** it is Br. Their bite angles (N(1)–Re(1)–N(2), average 75.2°) are significantly smaller than the ideal value of 90°, imposed by the rigid geometry of the chelating bipyridine ligands. In **5** and **6**, the π conjugation within the TTF unit is extended to all six sulfur atoms, and the central S_6C_8 moiety is very close to planar (Fig. 2). On the other hand, the C(15)–C(16) bond is significantly longer than the C(17)–C(18) bond, revealing the single-bond nature of the C(15)–C(16) bond. This precludes an extensive π-conjugation between the bipy and TTF units. There is no significant difference between the three Re–C distances in complex **5**. Nevertheless, for **6**, the bond Re(1)–C(2) *trans* to Br(1) with 1.802(13) Å is much shorter than the other two Re–C bonds *trans* to the pyridine nitrogen (1.952(15) Å and 1.984(5) Å). This can be explained by the

increased π-donor ability of bromide compared with chloride, which results in a stronger π-back-bonding to the trans-CO. Additionally, it is noted the significant difference between the bond angles of Re–C≡O in complexes **5** and **6**. The three carbonyl groups for **5** are almost linear with 175.4–178°, whereas the carbonyl group of the complex **6** trans to Br is significantly twisted (159°).

2.3. Electronic absorption and emission

The absorption spectra of compounds L^1, L^2 and **1**–**8** were measured, and the absorption data were summarized in Table 3.

As shown in Fig. 3, the absorption spectra of compounds L^1 and **1**–**4** consist of several absorption bands in the 250–500 nm spectral region, while the absorptions of compounds L^2 and **5**–**8** are in the range of 250–600 nm. The intense bands of the rhenium complexes, related to intraligand (π–π^*) transitions, are observed in the UV spectral region (<360 nm). At lower energy, all complexes exhibit the absorptions of a metal-to-ligand charge-transfer $d\pi(Re)$–$\pi^*(N$–$N)$ (MLCT) origin centered around 400 nm. Also, the MLCT transitions of the ester complexes may contain some interligand charge-transfer (ILCT) characters since the corresponding free ligands also absorb in the same region. With the same multi-sulfur ligand, the absorption bands of the chloride and bromide complexes have similar integrated peak areas. It is noted that MLCT absorptions observed for Re^I complexes with 1,3-dithiole core (**1**–**4**) are more intense than those for complexes with TTF unit (**5**–**8**), which is reasonable since complexes **14** have more conjugated π systems.

The absorption spectral changes of compounds L^2 and **5**–**8** upon addition of TCNQ were also investigated (Figs. 4, Figs. S2 and S3). In the presence of TCNQ, the ester ligand L^2 and its complexes exhibit an additional absorption shoulder at ca. 380 nm and the absorption intensities (320–440 nm) are significantly enhanced. In contrast, for the complexes containing carboxylic groups (**7** and **8**), the presence of TCNQ resulted in new absorption bands during 700–900 nm, which were not observed from the ester complexes. These results are consistent with the formation of charge-transfer complexes between the compounds containing electron-donor TTF unit and the classical electron-acceptor TCNQ during the titration of compounds **7** and **8**.

The normalized emission spectra of **3** and **4** in CH_3OH, **5** and **6** in CH_2Cl_2 are shown in Fig. 5. For **3** and **4**, excitation at the MLCT absorption region (∼440 nm) leads to blue emissions (∼480 nm) at room temperature, which may be attributed to ligand-centred π^*–π relaxations. While photoexcitation of **5** and **6** at RT at ca. 460 nm gives rise to red emissions (∼610 nm), the characteristic MLCT emissions of Re^I complexes [18,36–39]. No detectable emission for complexes **1**, **2**, **7**, and **8** was observed at the same conditions.
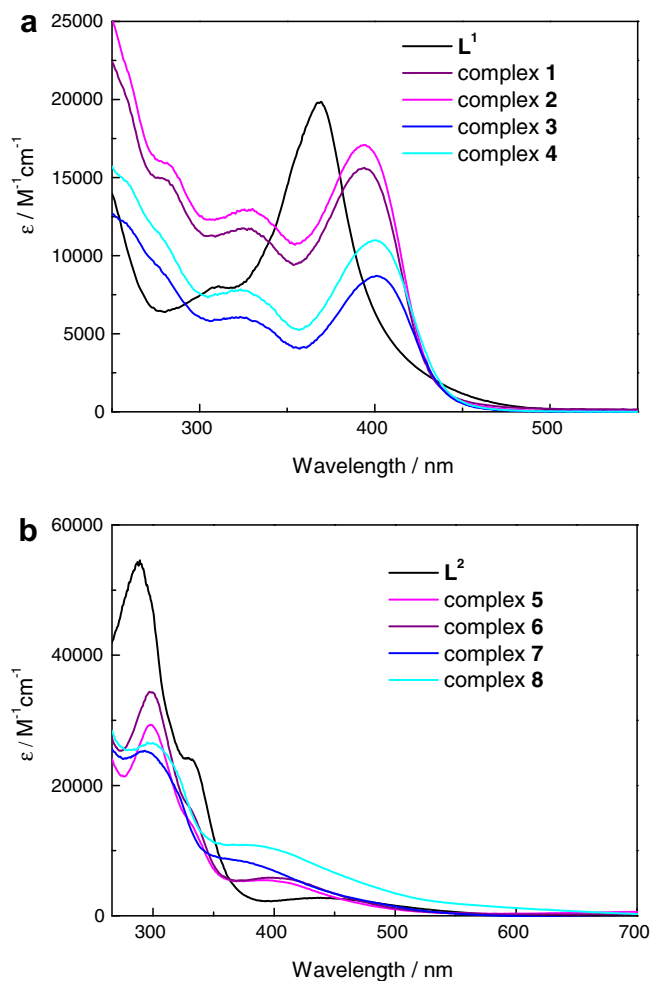

Fig. 3. Electronic absorption spectra of (a) compounds L^1 and 1–4; (b) compounds L^2 and 5–8.
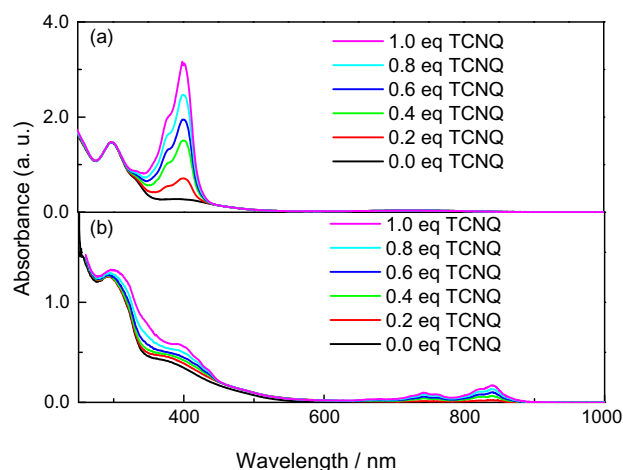
Fig. 4. UV–Vis absorption spectra of (a) complex **5** in 5×10^{-5} M CH_2Cl_2; (b) complex **7** in 5×10^{-5} M CH_3OH-DMF mixed solvent (v/v, 9:1) in the presence of varying amounts of TCNQ.

2.4. Electrochemistry

Oxidation–reduction processes were determined by cyclic voltammetry, and potentials are listed in Table 4. The representative

Table 3
Absorption[a] and emission[b] data of compounds L^1, L^2 and **1**–**8**.

Compound	Medium	Abs [λ, nm (ε, M^{-1} cm^{-1})]	λ_{em} (nm)
L^1	CH_2Cl_2	311sh (8042), 367 (19788)	–
1	CH_2Cl_2	279 (14976), 328 (11740), 394 (15636)	–
2	CH_2Cl_2	281 (15936), 328 (12954), 394 (17094)	–
3	CH_3OH	323 (6080), 401 (8710)	483
4	CH_3OH	324 (7846), 400 (10986)	479
L^2	CH_2Cl_2	289 (54572), 330sh (24232)	–
5	CH_2Cl_2	298 (29334), 398 (5432)	609
6	CH_2Cl_2	297 (34398), 400 (5842)	612
7	CH_3OH:DMF (v/v, 9:1)	293 (25336), 377 (8300)	–
8	CH_3OH:DMF (v/v, 9:1)	295 (26594), 376 (10892)	–

[a] The absorption data were obtained in 5×10^{-5} M solution.
[b] Complexes **1**, **2**, **7**, **8** and the free ligands L^1 and L^2 have no obvious emission.

Fig. 5. Normalized emission spectra of **3** and **4** in CH₃OH; **5** and **6** in CH₂Cl₂.
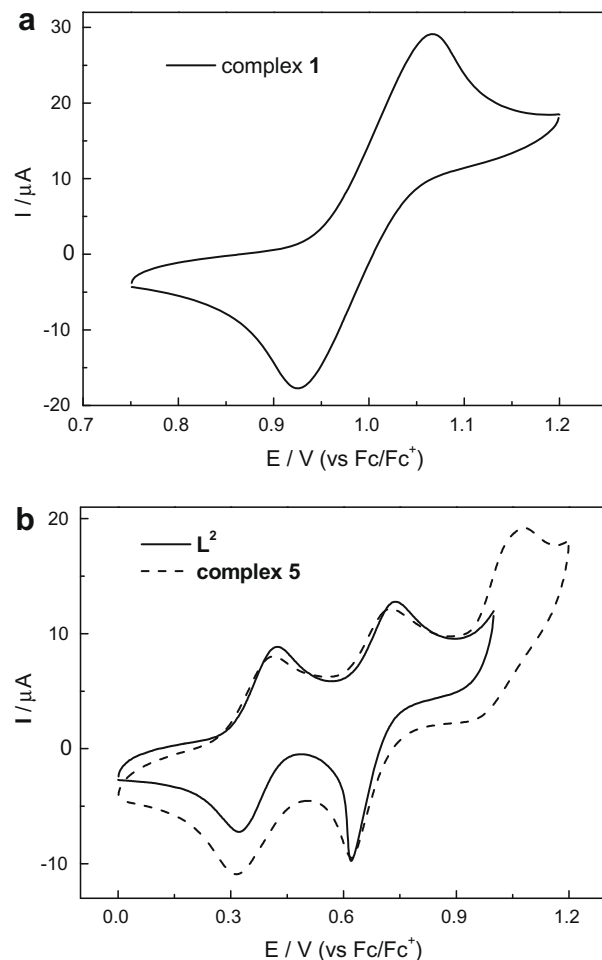

Fig. 6. CV results for (a) complex **1**; (b) compounds L^2 and **5** in 5×10^{-4} M CH₂Cl₂, at a scan rate of 100 mV s⁻¹ with n-Bu₄NClO₄ (0.1 M) as the supporting electrolyte.

cyclic voltammograms of **1**, L^2, and **5** are shown in Fig. 6, and the results of **3** and **8** are shown in Figs. S4 and S5, respectively.

Complexes **1** and **2** display one quasi-reversible wave occurred at 1.00 V (vs. Fc/Fc⁺), while **3** and **4** show an irreversible wave at 0.82 V (vs. Fc/Fc⁺), which are all assigned to a Re^I-based oxidation process (Re^I/Re^II) [6,36–39]. Complexes **5** and **6** exhibit an irreversible oxidation wave at 1.08 V (vs. Fc/Fc⁺), and two reversible one-electron redox couples at $E_{1/2}^1 = 0.36-0.37$ V and $E_{1/2}^2 = 0.67-0.68$ V (vs. Fc/Fc⁺), respectively. The first oxidation at higher potential position is associated with a metal-centered reaction from Re^I to Re^II. The other two redox couples are related to the ligand-based process, a typical property of TTF derivatives. Complexes **7** and **8** only show an irreversible wave of Re^I/Re^II at 1.10 V (vs. Fc/Fc⁺) [60].

2.5. Photovoltaic performance

Preliminary studies of the photovoltaic properties for **3**, **4**, **7** and **8** were also performed. Fig. 7 shows the photocurrent density-voltage characteristic curves of **3**, **4**, **7**, and **8** sensitized solar cells. The photovoltaic parameters of the cells sensitized with the above compounds are summarized in Table 5. Herein, Re(CO)₃(H₂d-pydt)Br (**4**) exhibits the relatively better photovoltaic performance. The short-circuit photocurrent density (J_{sc}), open-circuit photo-voltage (V_{oc}), fill factor (FF) and overall conversion efficiency (η) are 1.53 mA/cm², 430 mV, 0.73 and 0.48%, respectively. At the same experimental conditions, the films similarly impregnated with the classical dye N3 were measured for comparison

Table 4
Electrochemical data for compounds L^2 and **1**–**8**.

Compound	$E_{1/2}$ (V[a])		E (V[a])
	$L^{+/0}$	$L^{2+/+}$	Re^{2+/+}
1	–	–	1.00[b]
2	–	–	1.00[b]
3	–	–	0.82[b]
4	–	–	0.82[b]
L^2	0.37	0.68	–
5	0.36	0.67	1.08[c]
6	0.37	0.68	1.08[c]
7	–	–	1.10[c]
8	–	–	1.10[c]

[a] V vs. Fc/Fc⁺.
[b] $E = E_{1/2}$.
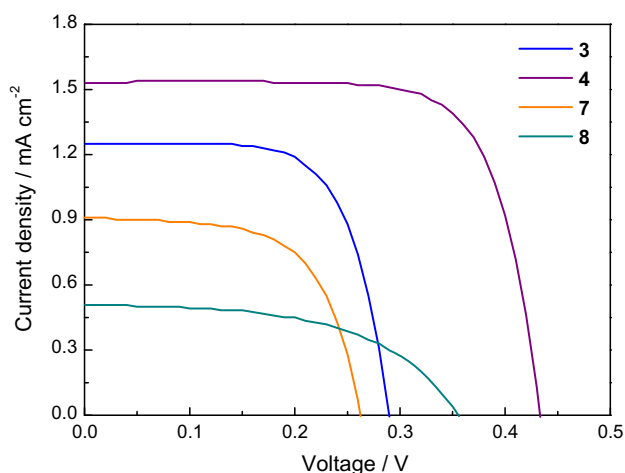[c] $E = E_p^{ox}$.

Fig. 7. Photocurrent density–voltage characteristic of photovoltaic device with complex Re(CO)₃(H₂dpydt)Cl (**3**), Re(CO)₃(H₂dpydt)Br (**4**), Re(CO)₃(H₂bpyTTF)Cl (**7**) and Re(CO)₃(H₂bpyTTF)Cl (**8**) as sensitizers.

($\eta \approx 5\%$). The absorption of these tricarbonyl rhenium(I) complexes are mainly in the blue and ultraviolet regions, which may lead to the poor harvesting of solar light reported herein [42].

Table 5
Photovoltaic parameters of the cells sensitized with complexes **3**, **4**, **7**, **8** and N3.[a]

Sensitizer	J_{sc} (mA/cm^2)	V_{oc} (mV)	FF	η (%)
N3	13.41	730	0.51	5.0
Re(CO)$_3$(H$_2$dpydt)Cl (**3**)	1.25	290	0.67	0.24
Re(CO)$_3$(H$_2$dpydt)Br (**4**)	1.53	430	0.73	0.48
Re(CO)$_3$(H$_2$bpyTTF)Cl (**7**)	0.91	260	0.61	0.15
Re(CO)$_3$(H$_2$bpyTTF)Br (**8**)	0.51	360	0.53	0.10

[a] These cells are fabricated and tested in the same experimental conditions.

3. Conclusions

We present here a detailed study on the syntheses and characterizations for rhenium tricarbonyl complexes of bispyridine ligands of either 1,3-dithiole or TTF pendant. The photochemical and electrochemical properties of both the free ligands and Re-complexes were studied. Very importantly, interesting rhenium complexes containing free carboxylic acid pendants were prepared, which enabled the incorporation of the new dyes into the solar cell devices. The performance of the complexes **3**, **4**, **7** and **8** as photosensitizers in the nanocrystalline TiO$_2$-based solar cell is relatively poor, which is likely due to the low light-harvesting efficiency of Re^I moiety. The results broaden the field of studies (especially on applications) on delocalized multi-sulfur ligands and rhenium(I) carbonyl complexes. More work is currently underway to explore new tricarbonyl rhenium complexes with different polypyridine and multi-sulfur derivatives, and to optimize their photovoltaic performance.

4. Experimental

4.1. General methods and materials

All reactions were performed under a nitrogen atmosphere using standard Schlenk line techniques. Re(CO)$_5$X (X = Cl and Br) and P(OEt)$_3$ were obtained from commercial sources and used without further purification. Dimethyl 2-(di(2-pyridyl)methylene)-1,3-dithiole-4,5-dicarboxylate (**L^1**) was prepared by the cross-coupling reaction from dimethyl 1,3-dithiole-2-thione-dicarboxylate and di-2-pyidyl ketone. The compounds 4,5-bis(methyloxycarbonyl)-1,3-dithio-2-one (**IIa**) and 4, 5-[(4′-methyl-2,2′-dipyrid-4-yl) ethylenedithio]-1,3-dithiole-2-thione (**IIb**) were synthesized with the reported procedure [61,62]. ^{1}H NMR spectra were recorded on a Bruker AM 500 spectrometer. Infrared spectroscopy was performed on a Vector22 Bruker Spectrophotometer (400-4000 cm^{-1}) with KBr pellets. UV–Vis spectra were recorded on a UV-3100 spectrophotometer. Emission spectra were carried out on AMINCO Bowman Series 2 Luminescence Spectrometer in a 1-cm quartz cell. Mass spectra were collected using a Bruker Autoflex II TOF/TOF spectrometer. Elemental analyses for C, H, and N were measured on a Perkin–Elmer 240C analyzer. Cyclic voltammetry (CV) experiments were performed on a CHI660b electrochemistry workstation with a three-electrode system. A glassy carbon electrode, platinum wire and Ag/AgNO$_3$/acetonitrile (10 mM) were used as the working, auxiliary, and reference electrode, respectively. CV measurements were made in CH$_2$Cl$_2$ or DMF solution with 0.1 M tetrabutylammonium perchlorate as supporting electrolyte.

4.1.1. Synthesis of Re(CO)$_3$(Medpydt)Cl (**1**)

Under a nitrogen atmosphere, Re(CO)$_5$Cl (108 mg, 0.3 mmol) and **L^1** (116 mg, 0.3 mmol) were refluxed in 15 mL of toluene for 1.5 h. The obtained mixture was cooled, and the yellow precipitate was filtered and washed with n-hexane (175 mg, 84%). IR (KBr) (ν_{max}, cm^{-1}): 2020, 1929, 1896 ($\nu_{C\equiv O}$). ^{1}H NMR (500 MHz, CDCl$_3$, δ): 9.15 (d, J = 5.2 Hz, 2H), 7.93 (d, J = 7.1 Hz, 2H), 7.79 (d, J = 7.6 Hz, 2H), 7.40 (t, 2H), 3.88 (s, 6H). MS (MALDI-TOF): m/z: 657.1 ([M−Cl]$^+$). Anal. Calc. for ReC$_{21}$H$_{14}$N$_2$O$_7$S$_2$Cl: C, 36.44; H, 2.04; N, 4.05. Found: C, 36.31; H, 2.02; N, 4.01%.

4.1.2. Synthesis of Re(CO)$_3$(Medpydt)Br (**2**)

Compound **2** was obtained by a method similar to the preparation of **1** using Re(CO)$_5$Br instead of Re(CO)$_5$Cl. Yield: 83%. IR (KBr) (ν_{max}, cm^{-1}): 2017, 1894 ($\nu_{C\equiv O}$). ^{1}H NMR (500 MHz, CDCl$_3$, δ): 9.27 (d, J = 5.0 Hz, 2H), 7.92 (d, J = 7.7 Hz, 2H), 7.79 (d, J = 7.8 Hz, 2H), 7.39 (t, 2H), 3.88 (s, 6H). MS (MALDI-TOF): m/z: 656.2 ([M−Br]$^+$). Anal. Calc. for ReC$_{21}$H$_{14}$N$_2$O$_7$S$_2$Br: C, 34.24; H, 1.92; N, 3.80. Found: C, 34.28; H, 1.85; N, 3.74%.

4.1.3. Synthesis of Re(CO)$_3$(H$_2$dpydt)Cl (**3**)

To a solution of **1** (90 mg, 0.13 mmol) in THF (10 mL), an aqueous solution of KOH was added and adjusted to pH 9–10. After the mixture was stirred for 1 h at room temperature, the solution was concentrated under vacuum, and then adjusted to pH 3 with acetic acid. A yellow precipitate was obtained, filtered and dried in vacuum to provide **3** (68 mg, 79%). IR (KBr) (ν_{max}, cm^{-1}): 2019, 1911, 1894 ($\nu_{C\equiv O}$). ^{1}H NMR (500 MHz, DMSO-d_6, δ): 8.89 (d, J = 4.5 Hz, 2H), 8.16 (t, 2H), 8.03 (d, J = 7.5 Hz, 2H), 7.59 (d, J = 5.5 Hz, 2H). MS (MALDI-TOF): m/z: 629.1 ([M−Cl]$^+$). Anal. Calc. for ReC$_{19}$H$_{10}$N$_2$O$_7$S$_2$Cl: C, 34.36; H, 1.52; N, 4.22. Found: C, 34.22; H, 1.59; N, 4.17%.

4.1.4. Synthesis of Re(CO)$_3$(H$_2$dpydt)Br (**4**)

Compound **4** was obtained by a method similar to the preparation of **3** using **2** instead of **1**. Yield: 77%. IR (KBr) (ν_{max}, cm^{-1}): 2018, 1911, 1897 ($\nu_{C\equiv O}$). ^{1}H NMR (500 MHz, DMSO-d_6, δ): 9.01 (d, J = 4.7 Hz, 2H), 8.17 (t, 2H), 8.03 (d, J = 7.7 Hz, 2H), 7.58 (t, 2H). MS (MALDI-TOF): m/z: 629.0 ([M−Br]$^+$). Anal. Calc. for ReC$_{19}$H$_{10}$N$_2$O$_7$S$_2$Br: C, 32.21; H, 1.42; N, 3.95. Found: C, 32.09; H, 1.47; N, 3.88%.

4.1.5. Synthesis of 4,5-bis(methyloxycabonyl)-4′,5′-(4′-methyl-2,2′-dipyrid-4-ylethylenedithio)-tetrathiafulvalene (MebpyTTF, **L^2**)

A suspension of **IIa** (281 mg, 1.2 mmol) and **IIb** (470 mg, 1.2 mmol) in 5 mL of P(OEt)$_3$ under nitrogen was heated to 120 °C and stirred for 3 h. After cooling to room temperature, a red precipitate was formed. Pure red compound **L^2** was isolated after separation by silica gel column chromatography with CH$_2$Cl$_2$/Et$_2$O (5:1) (170 mg, 24.5%). IR (KBr) (ν_{max}, cm^{-1}): 1719 ($\nu_{C=O}$). ^{1}H NMR (500 MHz, CDCl$_3$, δ): 8.72 (d, J = 4.5 Hz, 1H), 8.58 (d, J = 4.0 Hz, 1H), 8.50 (s, 1H), 8.31 (s, 1H), 7.38 (s, 1H), 7.24 (s, 1H), 4.78 (d, J = 6.0 Hz, 1H), 3.87 (s, 6H), 3.54 (m, 2H), 2.50 (s, 3H). MS (MALDI-TOF): m/z: 578.1 (M$^+$). Anal. Calc. for C$_{23}$H$_{18}$N$_2$O$_4$S$_6$: C, 47.73; H, 3.13; N, 4.84. Found: C, 47.77; H, 3.04; N, 4.78%.

4.1.6. Synthesis of Re(CO)$_3$(MebpyTTF)Cl (**5**)

Under a nitrogen atmosphere, Re(CO)$_5$Cl (73 mg, 0.2 mmol) and **L^2** (116 mg, 0.2 mmol) were refluxed in 10 mL of toluene for 2 h. The reaction mixture was concentrated, and pure orange compound **5** was isolated after separation by silica gel column chromatography (145 mg, 82%). IR (KBr) (ν_{max}, cm^{-1}): 2020, 1921, 1875 ($\nu_{C\equiv O}$). ^{1}H NMR (500 MHz, CDCl$_3$, δ): 9.01 (d, J = 5.5 Hz, 1H), 8.89 (d, J = 4.0 Hz, 1H), 8.21 (s, 1H), 8.03 (s, 1H), 7.49 (d, J = 5.3 Hz, 1H), 7.38 (s, 1H), 4.88 (s, 1H), 3.87 (s, 6H), 3.42 (m, 2H), 2.60 (s, 3H). MS (MALDI-TOF): m/z: 883.9 (M$^+$), 849.0 ([M−Cl]$^+$). Anal. Calc. for ReC$_{26}$H$_{18}$N$_2$O$_7$S$_6$Cl: C, 35.31; H, 2.05; N, 3.17. Found: C, 35.41; H, 2.08; N, 3.20%.

4.1.7. Synthesis of Re(CO)₃(MebpyTTF)Br (6)

Pure product of **6** was obtained by a method similar to the preparation of **5** using Re(CO)₅Br instead of Re(CO)₅Cl. Yield: 86%. IR (KBr) (v_{max}, cm^{-1}): 2020, 1913, 1894 ($v_{C\equiv O}$). ^{1}H NMR (500 MHz, CDCl₃, δ): 9.03 (d, J = 5.3 Hz, 1H), 8.91 (d, J = 4.9 Hz, 1H), 8.22 (s, 1H), 8.04 (s, 1H), 7.49 (d, J = 4.7 Hz, 1H), 7.38 (d, J = 4.3 Hz, 1H), 4.90 (s, 1H), 3.87 (s, 6H), 3.44 (m, 2H), 2.61 (s, 3H). MS (MALDI-TOF): m/z: 927.0 (M^{+}). Anal. Calc. for ReC₂₆H₁₈N₂O₇S₆Br: C, 33.62; H, 1.95; N, 3.02. Found: C, 33.54; H, 1.91; N, 3.00%.

4.1.8. Synthesis of Re(CO)₃(H₂bpyTTF)Cl (7)

Compound **7** was prepared by a method similar to the preparation of **3** using **5** instead of **1**. Yield: 78%. IR (KBr) (v_{max}, cm^{-1}): 2017, 1911, 1895 ($v_{C\equiv O}$). ^{1}H NMR (500 MHz, DMSO-d_6, δ): 9.01 (d, J = 5.6 Hz, 1H), 8.90 (d, J = 5.5 Hz, 1H), 8.84 (t, 1H), 8.75 (d, J = 6.2 Hz, 1H), 7.78 (d, J = 5.4 Hz, 1H), 7.61 (d, J = 5.5 Hz, 1H), 5.31 (s, 1H), 3.51 (m, 2H), 2.57 (s, 3H). MS (MALDI-TOF): m/z: 859.4 (M^{+}). Anal. Calc. for ReC₂₄H₁₄N₂O₇S₆Cl: C, 33.66; H, 1.65; N, 3.27. Found: C, 33.53; H, 1.73; N, 3.24%.

4.1.9. Synthesis of Re(CO)₃(H₂bpyTTF)Br (8)

Compound **8** was synthesized by a method similar to the preparation of **3** using **6** instead of **1**. Yield: 75%. IR (KBr) (v_{max}, cm^{-1}): 2019, 1908 ($v_{C\equiv O}$). ^{1}H NMR (500 MHz, DMSO-d_6, δ): 9.03 (d, J = 5.7 Hz, 1H), 8.90 (d, J = 5.5 Hz, 1H), 8.85 (t, 1H), 8.75 (d, J = 6.3 Hz, 1H), 7.74 (d, J = 5.4 Hz, 1H), 7.57 (d, J = 5.5 Hz, 1H), 5.31 (s, 1H), 3.51 (m, 2H), 2.64 (s, 3H). Anal. Calc. for ReC₂₄H₁₄N₂O₇S₆Br: C, 32.00; H, 1.57; N, 3.11. Found: C, 31.89; H, 1.62; N, 3.03%.

4.2. Crystal structure determination

Crystals of **1** · 2H₂O suitable for X-ray structure analysis were grown from the slow evaporation of a CH₂Cl₂ solution. For complexes **5** and **6**, single crystals were obtained from dichloromethane/diethyl ether. The data were collected on a Bruker Smart Apex CCD diffractometer equipped with graphite-monochromated Mo Kα (λ = 0.71073 Å) radiation using $\omega/2\theta$ scan mode at 293 K. The highly redundant data sets were reduced using SAINT and corrected for Lorentz and polarization effects. Absorption corrections were applied using SADABS supplied by Bruker. The structure was solved by direct methods and refined by full-matrix least-squares methods on F^2 using SHELXTL-97. All non-hydrogen atoms were found in alternating difference Fourier syntheses and least-squares refinement cycles and, during the final cycles, refined anisotropically. Hydrogen atoms were placed in calculated position and refined as riding atoms with a uniform value of U_{iso}.

4.3. Preparation of TiO₂ films and photoelectrochemical measurements

The photovoltaic properties are preliminarily investigated. The TiO₂ films were prepared using published procedures [63]. Photoelectrochemical data were measured using a 150 W tungsten halogen lamp that was focused to give 620 W/m^2 at the surface of the test cell. The applied potential and measured cell current was measured using a Keithley model 236 digital source meter. The dye solution was prepared in HPLC ethanol (5×10^{-4} M), and the electrolyte was composed of 0.5 mmol/L of dimethylhexylimidazolium, 20 mmol/L of iodine (I₂), 40 mmol/L of lithium iodide (LiI), and 500 mmol/L of *tert*-butylpyridine in acetonitrile.

Acknowledgments

Appendix A. Supplementary material

CCDC 690025, 690026 and 690027 contain the supplementary crystallographic data for **1**, **5** and **6**. These data can be obtained free of charge from The Cambridge Crystallographic Data Centre via www.ccdc.cam.ac.uk/data_request/cif. Supplementary data associated with this article can be found, in the online version, at doi:10.1016/j.jorganchem.2008.12.018.

References

[1] B.P. Sullivan, T.J. Meyer, J. Chem. Soc., Chem. Commun. (1984) 1244.
[2] J.V. Caspar, B.P. Sullivan, T.J. Meyer, Organometallics 5 (1986) 1500.
[3] J.V. Caspar, T.J. Meyer, J. Phys. Chem. 87 (1983) 952.
[4] C. Köllner, B. Pugin, A. Togni, J. Am. Chem. Soc. 120 (1998) 10274.
[5] H. Tsubaki, S. Tohyama, K. Koike, H. Saitoh, O. Ishitani, J. Chem. Soc., Dalton Trans. (2005) 385.
[6] H. Tsubaki, A. Sekine, Y. Ohashi, K. Koike, H. Takeda, O. Ishitani, J. Am. Chem. Soc. 127 (2005) 15544.
[7] K.K.-W. Lo, W.-K. Hui, C.-K. Chung, K.H.-K. Tsang, T.K.-M. Lee, C.-K. Li, J.S.-Y. Lau, D.C.-M. Ng, Coord. Chem. Rev. 250 (2006) 1724.
[8] J.C. Ostrowski, M.R. Robinson, A.J. Heeger, G.C. Bazan, Chem. Commun. (2002) 784.
[9] D.K. Rayabarapu, B.M.J.S. Paulose, J.-P. Duan, C.-H. Cheng, Adv. Mater. 17 (2005) 349.
[10] Y.-Y. Lyu, Y. Byun, O. Kwon, E. Han, W.S. Jeon, R.R. Das, K. Char, J. Phys. Chem. B 110 (2006) 10303.
[11] S.-Y. Chang, J. Kavitha, S.-W. Li, C.-S. Hsu, Y. Chi, Y.-S. Yeh, P.-T. Chou, G.-H. Lee, A.J. Carty, Y.-T. Tao, C.-H. Chien, Inorg. Chem. 45 (2006) 137.
[12] S. Bernhard, X. Gao, G.G. Malliaras, H.D. Abruna, Adv. Mater. 14 (2002) 433.
[13] M.H. Keefe, K.D. Benkstein, J.T. Hupp, Coord. Chem. Rev. 205 (2000) 201.
[14] A.J. DiBilio, B.R. Crane, W.A. Wehbi, C.N. Kiser, M.M. Abu-Omar, R.M. Carlos, J.H. Richards, J.R. Winkler, H.B. Gray, J. Am. Chem. Soc. 123 (2001) 3181.
[15] N.J. Lundin, A.G. Blackman, K.C. Gordon, D.L. Officer, Angew. Chem., Int. Ed. 45 (2006) 2582.
[16] S.Y. Reece, M.R. Seyedsayamdost, J. Stubbe, D.G. Nocera, J. Am. Chem. Soc. 128 (2006) 13654.
[17] M.H.W. Lam, D.Y.K. Lee, K.W. Man, C.S.W. Lau, J. Mater. Chem. 10 (2000) 1825.
[18] V.W.-W. Yam, K.-Z. Wang, C.-R. Wang, Y. Yang, K.-K. Cheung, Organometallics 17 (1998) 2440.
[19] A.J. Lees, Chem. Rev. 87 (1987) 711.
[20] M.K. Nazeeruddin, C. Klein, P. Liska, M. Grätzel, Coord. Chem. Rev. 249 (2005) 1460.
[21] L.D. Ciana, W.J. Dressicak, D. Sandrini, M. Maestri, M. Ciano, Inorg. Chem. 29 (1990) 2792.
[22] T.J. Meyer, Pure Appl. Chem. 58 (1986) 1193.
[23] E.M. Kober, J.L. Marshall, W.J. Dressick, B.P. Sullivan, J.V. Caspar, T.J. Meyer, Inorg. Chem. 24 (1985) 2755.
[24] R. Argazzi, N.Y.M. Iha, H. Zabri, F. Odobel, C.A. Bignozzi, Coord. Chem. Rev. 248 (2004) 1299.
[25] B. O'Regan, M. Grätzel, Nature 353 (1991) 737.
[26] C.-Y. Chen, S.-J. Wu, C.-G. Wu, J.-G. Chen, K.-C. Ho, Angew. Chem., Int. Ed. 45 (2006) 5822.
[27] P. Wang, C. Klein, R. Humphry-Baker, S.M. Zakeeruddin, M. Grätzel, J. Am. Chem. Soc. 127 (2005) 808.
[28] A. Kukrek, D. Wang, Y. Hou, R. Zong, R. Thummel, Inorg. Chem. 45 (2006) 10131.
[29] M.K. Nazeeruddin, P. Péchy, T. Renouard, S.M. Zakeeruddin, R. Humphry-Baker, P. Comte, P. Liska, L. Cevey, E. Costa, V. Shklover, L. Spiccia, G.B. Deacon, C.A. Bignozzi, M. Grätzel, J. Am. Chem. Soc. 123 (2001) 1613.
[30] C.-Y. Chen, H.-C. Lu, C.-G. Wu, J.-G. Chen, K.-C. Ho, Adv. Funct. Mater. 17 (2007) 29.
[31] P.-H. Xie, Y.-J. Hou, B.-W. Zhang, Y. Cao, F. Wu, W.-J. Tian, J.-C. Shen, J. Chem. Soc., Dalton Trans. (1999) 4217.
[32] T. Horiuchi, H. Miura, K. Sumioka, S. Uchida, J. Am. Chem. Soc. 126 (2004) 12218.
[33] K.S. Schanze, D.B. MacQueen, T.A. Perkins, L.A. Caban, Coord. Chem. Rev. 122 (1993) 63.
[34] D.J. Stufkens, A. Vlček Jr., Coord. Chem. Rev. 177 (1998) 127.
[35] D.R. Striplin, G.A. Crosby, Coord. Chem. Rev. 211 (2001) 163.
[36] Z. Si, J. Li, B. Li, F. Zhao, S. Liu, W. Li, Inorg. Chem. 46 (2007) 6155.
[37] K. Wang, L. Huang, L. Gao, L. Jin, C. Huang, Inorg. Chem. 41 (2002) 3353.
[38] V.W.-W. Yam, S.H.-F. Chong, C.-C. Ko, K.K. Cheung, Organometallics 19 (2000) 5092.
[39] S.-S. Sun, A.J. Lees, Organometallics 20 (2001) 2353.
[40] V. Balzani, A. Juris, M. Venturi, S. Campagna, S. Serroni, Chem. Rev. 96 (1996) 759.
[41] L.A. Worl, R. Duesing, P. Chen, L.D. Ciana, T.J. Meyer, J. Chem. Soc., Dalton Trans. (1991) 849.

[42] G.M. Hasselmann, G.J. Meyer, J. Phys. Chem. B 103 (1999) 7671.
[43] Q.-Y. Zhu, J. Dai, D.-X. Jia, L-H. Cao, H.-H. Lin, Eur. J. Inorg. Chem. (2004) 4789.
[44] S.A. Baudron, M.W. Hosseini, Inorg. Chem. 45 (2006) 5260.
[45] K. Sako, Y. Misaki, M. Fujiwara, T. Maitani, K. Tanaka, H. Tatemitsu, Chem. Lett. (2002) 592.
[46] K. Takahashi, T. Kawakami, Z.-Z. Gu, Y. Einaga, A. Fujishima, O. Sato, Chem. Commun. (2003) 2374.
[47] A. Staniszewski, W.B. Heuer, G.J. Meyer, Inorg. Chem. 47 (2008) 7062.
[48] W. Liu, R. Wang, X.-H. Zhou, J.-L. Zuo, X.-Z. You, Organometallics 27 (2008) 126.
[49] W. Liu, Y. Chen, R. Wang, X.H. Zhou, J.L. Zuo, X.Z. You, Organometallics 27 (2008) 2990.
[50] E. Coronado, C.J. Gómez-García, Chem. Rev. 98 (1998) 273.
[51] M.R. Bryce, Adv. Mater. 11 (1999) 11.
[52] L. Ouahab, T. Enoki, Eur. J. Inorg. Chem. (2004) 933.
[53] J.L. Segura, N. Martín, Angew. Chem., Int. Ed. 40 (2001) 1372.
[54] M.R. Bryce, J. Mater. Chem. 5 (1995) 1469.
[55] T. Enoki, A. Miyazaki, Chem. Rev. 104 (2004) 5449.
[56] Y. Ji, R. Zhang, Y.-J. Li, Y.-Z. Li, J.-L. Zuo, X.-Z. You, Inorg. Chem. 46 (2007) 866.
[57] S.A. Moya, R. Schmidt, R. Pastene, R. Sartori, U. Müller, G. Frenzen, Organometallics 15 (1996) 3463.
[58] S.R. Banerjee, M.K. Levadala, N. Lazarova, L. Wei, J.F. Valliant, K.A. Stephenson, J.W. Babich, K.P. Maresca, J. Zubieta, Inorg. Chem. 41 (2002) 6417.
[59] E.W. Abel, K.G. Ouell, A.G. Osborne, H.M. Pain, V. Sik, M.B. Hursthouse, K.M.A. Malik, J. Chem. Soc., Dalton Trans. (1994) 3441.
[60] B.J. Coe, N.R.M. Curati, E.C. Fitzgerald, S.J. Coles, P.N. Horton, M.E. Light, M.B. Hursthouse, Organometallics 26 (2007) 2318.
[61] R.P. Parg, J.D. Kilburn, M.C. Petty, C. Pearson, T.G. Ryan, Synthesis (1994) 613.
[62] K. Hervé, S.-X. Liu, O. Cador, S. Golhen, Y.L. Gal, A. Bousseksou, H. Stoeckli-Evans, S. Decurtins, L. Ouahab, Eur. J. Inorg. Chem. (2006) 3498.
[63] P. Wang, S.M. Zakeeruddin, P. Comte, R. Charvet, R. Humphry-Baker, M. Grätzel, J. Phys. Chem. B 107 (2003) 14336.